Research Article

Developing the analytical solution for the nonlinear bioheat transfer equation through homotopy analysis method along with an optimal convergence-control parameter

Rouhollah OSTADHOSSEIN[1],*

[1]Department of Mechanical Engineering, West Tehran Branch, Islamic Azad University, Tehran, P8WP+RV3, Iran

ABSTRACT

The Homotopy Analysis Method (HAM) is an effective technique to achieve the analytical solution of a broad range of problems, mainly with nonlinear governing equations. The solution of Pennes' bioheat equation in nonlinear form arising from the linear temperature-dependent nature of specific heat capacity of a biological tissue using the Homotopy Analysis Method has been obtained analytically and validated with the numerical results obtained from the Finite Difference Method (FDM) the first time in this study. The analysis demonstrated that considering the various values of the convergence parameter and computing the Mean Squared Error (MSR) to achieve the optimum values ensures accurate results even at the low-order approximations of the solution. Investigating the effect of the nonlinear term's magnitude on the solution indicated a direct relationship; However, the effect was not remarkable even at the major values, thus it is possible to consider the specific heat capacity of a living tissue, a constant value through thermal simulations. According to this research, the Homotopy Analysis Method can be a proper method to derive the analytical solution of either the linear or nonlinear form of Pennes' bioheat equation.

Cite this article as: Ostadhossein R. Developing the analytical solution for the nonlinear bioheat transfer equation through homotopy analysis method along with an optimal convergence-control parameter. J Ther Eng 2024;10(3):613–621.

INTRODUCTION

Mathematical modeling of the heat transfer phenomenon within biological tissues has been a fascinating problem to scientists and mathematicians for over seventy years, dating back to Harry H. Pennes' attempt to formulate bioheat transfer along the human forearm for the first time in 1948 [1]. Various models have been suggested for the heat transfer phenomenon inside living tissues since then. However, Pennes' equation has remained the most extensively applied mathematical formulation to study the bioheat transfer phenomenon [2]. The solution of Pennes' bioheat equation into a semi-infinite tissue was offered analytically by Shih et al. employing the Laplace transform. The heat flux followed a sinusoidal function. Shahnazari et al. found the solution of this equation for the skin exposed to a frequent

*Corresponding author.
*E-mail address: sepehr.ost@gmail.com

thermal flux. A procedure based on the Weighted Residual and Homotopy Perturbation Method (HPM) was applied to achieve the results [3,4]. Qin and Wu solved the Pennes' bioheat equation fractional form numerically by applying the quadratic spline collection method, whereas Al-Humedi and Al-Saadawi introduced the answer numerically using the shifted Legendre polynomials. Liu and Tu suggested the numerical results for Pennes' differential equation including transient blood temperature through the Laplace transform [5-7]. A mathematical model to present the space-fractional form of this equation was proposed by Singh et al. The solution was achieved using HPM after turning it into an IVP. Kumar et al. obtained the answer numerically utilizing the Finite Difference Method (FDM) and the Legendre wavelet Galerkin procedure. In contrast, Wang et al. developed a model for the bioheat transfer during laser irradiation based on non-Fourier heat conduction. In the following, Kabiri and Talaee solved Pennes' bioheat equation in hyperbolic form, subject to a mobile heat source analytically based on the Eigenvalue Method [8-11]. The Fibonacci wavelet method was applied to find the answer by Irfan et al. as a different approach. Time-fractional Pennes' equation solution was offered using the Fibonacci wavelet method by Irfan and Shah subsequently [12,13].

Lakhssassi et al. proposed a simplified formulation according to the modified format of this bioheat equation at the steady state. The solutions were found using the Weierstrass elliptic function. Gupta et al. presented a model for heat transfer within thermal therapy using electromagnetic radiation. The solution was achieved by the Galerkin method with the B-polynomial, and the problem was solved by HPM [14,15]. Majchrzak offered the solution by the Boundary Element Method (BEM) for a dual-phase-lag problem. Majchrzak and Turchan also obtained a three-dimensional solution to a similar problem by general BEM [16,17].

Numerous attempts have been made thus far in the pursuit of finding numerical and analytical solutions for nonlinear heat transfer equations [18-21]. Karimipour et al. conducted a study to investigate the effects of gravity on mixed convection heat transfer in a microchannel using the Lattice Boltzmann Method [22]. In similar research, the effects of magnetic field and slip were studied on the developing laminar forced convection of nanofluid in a microchannel [23]. Karimipour also conducted research on forced convection heat transfer of certain nanofluids in a microchannel using the Lattice Boltzmann Method (LBM) [24,25]. Menni et al. examined turbulent heat transfer and fluid flow over complex geometry fins [26]. Similarly, Menni et al. studied convection heat transfer in channels [27-29].

A practical technique of calculating the analytical results based on a power series named the Homotopy Analysis Method (HAM), was introduced by Liao in 1997 [30]. Being independent of small parameters is a significant superiority of this technique in comparison with perturbation methods. This method combines the classic perturbation and the homotopy of topology [31]. HAM was utilized to find the answer of nonlinear heat transfer problems by Abbasbandy. To validate the results, the solutions were compared with the results from Runge-Kutta and HPM [32].

Hariharan found the solution of some partial differential equations relevant to engineering problems, including linear non-homogeneous Cauchy differential equations by this method. A similar attempt was made to apply HAM to solving some nonlinear parabolic-hyperbolic Cauchy problems by Gupta and Gupta [33,34]. Lu and Liu investigated the application of HAM to investigate the results for the variable-coefficient form of the KdV-Burgers. Hesameddini and Latifizade also used this method to find the numerical solution for Painlevé equations with several initial conditions. HAM was used to study Magnetohydrodynamics (MHD) for free convection of a thin plate, which goes into a viscous fluid with low-heat resistance by Hammouch et al. [35-37]. Odibat presented an optimized kind of HAM. Biswal and Chakraverty studied the Jeffery-Hamel flow arising from the movement of a nanofluid inside a magnetic field by OHAM, and Obalalu et al. studied a Casson fluid flow applying HAM [38-40]. Rabbani introduced a modified HPM to obtain the answer for nonlinear integral equations. Jbr and Al-Rammahi used q-HAM to solve the Fredholm integral equation in nonlinear form. Abdulkhaleq applied a combination of HAM and the Harris Hawks method to solve several PDEs [41-43].

In this study, Pennes' bioheat equation with a nonlinear term arising from the linear temperature-dependent nature of the specific heat capacity of biological tissue has been solved using HAM for the first time. The accuracy was evaluated by comparing the results with the numerical answers derived from the Finite Difference Method (FDM) and calculating the Mean Squared Error.

PENNE'S BIOHEAT EQUATION

As it was mentioned in the introduction section, Penne's bioheat equation is the most common mathematical formulation for studying bioheat transfer. The Pennes' bioheat equation in general is shown in the form [44]:

$$\rho_t c_t \frac{\partial T}{\partial t} = \nabla.(k \nabla T) - \rho_b c_b \omega_p (T - T_a) + q_m \qquad (1)$$

By assuming a fixed thermal conductivity and blood perfusion rate for the biological tissue (k, $\omega_p = cte$) the one-dimensional form of (1) is derived as:

$$\rho_t c_t \frac{\partial T(x,t)}{\partial t} = k \frac{\partial^2 T(x,t)}{\partial x^2} - \rho_b c_b \omega_p (T(x,t) - T_a) + q_m \; ; 0 \leq x \leq L \qquad (2)$$

which x denotes the spatial variable of this equation. The initial condition of the equation is considered as:

$$T(x,0) = T_a \tag{3}$$

Defining the dimensionless groups below will result in the nondimensional form of (2).

$$X = \frac{x}{L}; \ \tau = t\,\omega_p; \ \theta = \frac{T}{T_a}; \ \alpha_1 = \frac{k}{\rho_t c_t \omega_p L^2};$$

$$\alpha_2 = \frac{\rho_b c_b}{\rho_t c_t}; \ \alpha_3 = \frac{1}{\rho_t c_t}\left(\rho_b c_b + \frac{q_m}{\omega_p T_a}\right) \tag{4}$$

The nondimensional form of (2) regarding the introduced dimensionless groups is:

$$\frac{\partial\theta(X,\tau)}{\partial\tau} = \alpha_1 \frac{\partial^2\theta(X,\tau)}{\partial X^2} - \alpha_2\,\theta(X,\tau) + \alpha_3; \ 0 \le X \le 1 \tag{5}$$

and the nondimensional initial condition is expressed as:

$$\theta(X,0) = 1 \tag{6}$$

Considering the tissue's specific heat capacity as the temperature's linear function, namely [45]:

$$c_t\left(T(x,t)\right) = c_0\left(1 + \beta\left(T(x,t) - T_a\right)\right) \tag{7}$$

and substituting it into (2) with the consideration of (8) results in (9). Here c_0 denotes the tissue's pecific heat capacity at core body temperature, and $\beta(\Theta^{-1})$ is a constant.

$$\varepsilon = \beta\,T_a \tag{8}$$

$$\left(1 + \varepsilon\left(\theta(X,\tau) - 1\right)\right)\frac{\partial\theta(X,\tau)}{\partial\tau} = \alpha_1 \frac{\partial^2\theta(X,\tau)}{\partial X^2} - \alpha_2\,\theta(X,\tau) \\ + \alpha_3; \ 0 \le X \le 1 \tag{9}$$

Homotopy Analysis Method (HAM)

Let us consider nonlinear Pennes' bioheat equation as follows [46]:

$$N[\theta(X,\tau)] = 0 \tag{10}$$

which N denotes the nonlinear operator, X and τ are the dimensionless spatial and temporal variables, and $\theta(X, \tau)$ is the unknown solution respectively. Assuming $\theta_0(X, \tau)$ as the initial guess, $h \ne 0$ the convergence-control parameter, $H(X, \tau) \ne 0$ the axillary function, and L the linear axillary operator with the character:

$$L(f) = 0 \quad \text{when} \quad f = 0 \tag{11}$$

and assuming $q \in [0,1]$, a homotopy is constructed as below:

$$(1-q)\{L[\Phi(X,\tau;q) - \theta_0(X,\tau)]\} = q\,h\,H(X,\tau)N[\Phi(X,\tau;q)] \tag{12}$$

When $q = 0$:

$$L[\Phi(X,\tau;0) - \theta_0(X,\tau)] = 0. \tag{13}$$

Referring to (11):

$$\Phi(X,\tau;0) = \theta_0(X,\tau) \tag{14}$$

When $q = 1$:

$$h\,H(X,\tau)N[\Phi(X,\tau;1)] = 0. \tag{15}$$

Since h, $H(X, \tau)$ are nonzero items, consequently:

$$N[\Phi(X,\tau;1)] = 0 \tag{16}$$

and this means:

$$\Phi(X,\tau;1) = \theta(X,\tau) \tag{17}$$

As it was demonstrated above, when q grows from 0 to 1, $\Phi(X, \tau; q)$ continuously converts from the initial guess into the analytical solution of nonlinear Pennes' bioheat equation which was introduced in (9). Expanding $\Phi(X, \tau; q)$ into the Tylor series respecting q results in the following equation:

$$\Phi(X,\tau;q) = \Phi(X,\tau;0) + \sum_{m=1}^{+\infty} \frac{1}{m!} \left.\frac{\partial^m \Phi(X,\tau;q)}{\partial q^m}\right|_{q=0.} q^m \tag{18}$$

By defining the m-th order deformation derivative in the form:

$$\theta_m(X,\tau) = \frac{1}{m!} \left.\frac{\partial^m \Phi(X,\tau;q)}{\partial q^m}\right|_{q=0} \tag{19}$$

$\Phi(X, \tau; q)$ is expanded in the following form, according to the Taylor expansion of $\Phi(X, \tau; q)$, which was shown in (18):

$$\Phi(X,\tau,q) = \theta_0(X,\tau) + \sum_{m=1}^{+\infty} \theta_m(X,\tau)\,q^m \tag{20}$$

Regarding (17) by setting $q = 1$ in (20), the solution of nonlinear Pennes' bioheat equation emerges as:

$$\theta(X,\tau) = \theta_0(X,\tau) + \sum_{m=1}^{+\infty} \theta_m(X,\tau) \tag{21}$$

The following vector is considered:

$$\vec{\theta}_n = \{\theta_0(X,\tau), \theta_1(X,\tau), \theta_2(X,\tau), \ldots, \theta_n(X,\tau)\} \tag{22}$$

To determine $\theta_m(X, \tau)$, the m-th order derivative of the zero-order deformation (12) with respect to q is computed, then the result is divided by $m!$ and finally q is set to 0. Through following this process, the high-order deformation appears in the form:

$$L[\theta_m(X,\tau) - \chi_m \theta_{m-1}(X,\tau)] = h H(X,\tau) R_m(\vec{\theta}_{m-1}, X, \tau) \quad (23)$$

and $\theta_m(X, \tau)$ is calculated as:

$$\theta_m(X,\tau) = \chi_m \theta_{m-1}(X,\tau) + h L^{-1}[H(X,\tau) R_m(\vec{\theta}_{m-1}, X, \tau)] \quad (24)$$

By introducing χ_m in the following form:

$$\chi_m = \begin{cases} 0 & m \leq 1 \\ 1 & m > 1 \end{cases} \quad (25)$$

and $R_m(\vec{\theta}_{m-1}, X, \tau)$ in the form:

$$R_m(\vec{\theta}_{m-1}, X, \tau) = \frac{1}{(m-1)!} \frac{\partial^{m-1}[\Phi(X,\tau;q)]}{\partial q^{m-1}} \bigg|_{q=0.} \quad (26)$$

besides substituting (25) and (26) into (24), $\theta(X, \tau)$ is calculated by (21). The m-th order approximation of $\theta(X, \tau)$ is presented as:

$$\theta(X,\tau) \approx \sum_{i=0}^{m} \theta_i(X,\tau) \quad (27)$$

The Analytical Solution Built on Homotopy Analysis Method

The analytical solution of (9) obtained by HAM has been investigated in this section. The boundary conditions in this article are defined as:

$$T(x,t)\big|_{x=0} = T_a \rightarrow \theta(X,\tau)\big|_{X=0} = 1 \quad (28)$$

$$T(x,t)\big|_{x=L} = 0 \rightarrow \theta(X,\tau)\big|_{X=1} = 0. \quad (29)$$

The linear operator is chosen $L = \dfrac{\partial(\,)}{\partial \tau}$, the nonlinear one is selected in the form $N = (1 + \varepsilon((\,)-1))\dfrac{\partial(\,)}{\partial \tau} - \alpha_1 \dfrac{\partial^2(\,)}{\partial X^2} + \alpha_2(\,) - \alpha_3$, and $H(X, \tau) = 1$ for simplification purposes here.

The initial guess is selected according to the boundary conditions (28), (29) as well as the right side of (9).

$$\frac{\partial}{\partial \tau}(\theta_0(X,\tau)) = 0 \rightarrow \theta_0(X) = -\frac{2\sinh(X)}{e - e^{-1}} + 1 \quad (30)$$

The m-th order approximation of the solution can be calculated referring to (24) with the boundary conditions below:

$$\theta_m(X,\tau)\big|_{X=0} = 0 \text{ and } \theta_m(X,\tau)\big|_{X=1} = 0. \quad (31)$$

A Maple code was written to implement the elaborated procedure and obtain the Pennes' nonlinear bioheat equation's analytical solution using HAM in this study.

RESULTS AND DISCUSSION

Assuming $\varepsilon = 1$, $\alpha_i = 1$ ($i = 1,2,3$), and following the described process will result in the m-th order approximate solution of (9) with the relevant boundary conditions. The zero and the first-order approximations are in the form:

$$\theta_0(X,\tau) = \frac{-e^{X+1} + e^{1-X} + e^2 - 1}{e^2 - 1} \quad (32)$$

$$\theta_1(X,\tau) = \frac{h\tau(-e^{-X+2} - e^{X+1} + e^{-X+1} + e^X + e^2)}{e^2 - 1}$$
$$+ \frac{e^{-X+1} - e^{X+1} + e^2 - h\tau - 1}{e^2 - 1} \quad (33)$$

Repeating this algorithm will result in higher-order deformations and more accurate approximations. It is evident that the first-order analytical solution and the numerical one achieved by the Finite Difference Method (FDM) converge at $h = 1.0$ with a remarkable level of accuracy as illustrated through Figure 1.

It is clear that the answer of (5) can be obtained by setting $\varepsilon = 0$. For the high computational cost of HAM in finding the higher-order approximate solutions of (9), the effect of the convergence parameter has only been studied on the
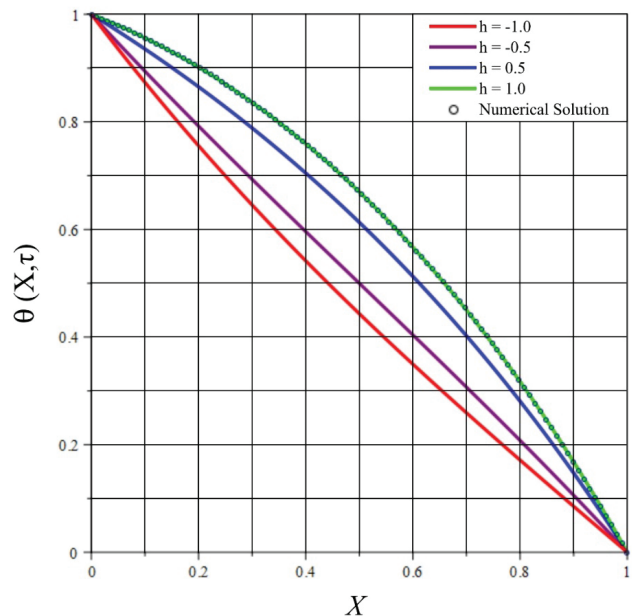
Figure 1. The first-order approximation of (9) at $\tau = 1$ with $\varepsilon = 1$, $\alpha_i = 1$ ($i = 1,2,3$) at various values of h in comparison with the answer derived from the Finite Difference Method (FDM).

first and second-order approximations at $\alpha_i = 1$ ($i = 1,2,3$), $\varepsilon = 1$, $\tau = 1$. The results have been noted in Tables 1 and 2. The Mean Squared Error (MSE) has been calculated in the following form for each h values [47]:

$$MSE = \frac{1}{4}\sum_{i=1}^{4}[\theta_{analytical}(X_i) - \theta_{numerical}(X_i)]^2 \quad (34)$$

MSE for the first and second-order approximations of the solution regarding the different h values has been depicted in Figure 2. It is easily recognized that with the increase of h, the error decreases gradually, and after a specific value, the error rises again. As can be observed, the optimum h values to achieve the least MSE for the first and second-order approximations, are 1.0 and 0.6 in order for the studied case. It demonstrates that by selecting an appropriate value for the convergence parameter, achieving accurate results even at low-order approximations is possible, and it is the superiority of HAM in comparison to other power- series-based analytical techniques.

The effect of ε on the second-order approximate solution with $h = 1.0$, $\tau = 1$ has been investigated and shown in Figure. 3. Since the small values of ε do not affect the solution remarkably, the results for the minor values have been indicated in Table 3. As can be recognized through the graph and table, the results grow with the increase in ε. The second-order approximate solutions of nonlinear Pennes' bioheat as a function of X, τ at $\varepsilon = 0, 20, 50, 100$, $\alpha_i = 1$ ($i = 1,2,3$), $h = 1.0$ for $0 \le X \le 1$ and $0 \le \tau \le 1$ have been displayed in Figure 4.

Table 1. MSE for the first-order approximate solution of (9) using HAM at the various h values

h	X1 = 0.2	X2 = 0.4	X3 = 0.6	X4 = 0.8	MSE
0.1	0.8359769521	0.6613577324	0.4691342585	0.2515919270	0.0068500091
0.2	0.8432743584	0.6722320648	0.4800085908	0.2588893330	0.0054568220
0.3	0.8505717646	0.6831063969	0.4908829230	0.2661867390	0.0042351383
0.4	0.8578691709	0.6939807291	0.5017572550	0.2734841460	0.0031849577
0.5	0.8651665773	0.7048550610	0.5126315880	0.2807815520	0.0023062804
0.6	0.8724639847	0.7157293950	0.5235059210	0.2880789590	0.0015991063
0.7	0.8797613910	0.7266037270	0.5343802530	0.2953763670	0.0010634354
0.8	0.8870587980	0.7374780600	0.5452545860	0.3026737740	0.0006992678
0.9	0.8943562030	0.7483523920	0.5561289180	0.3099711780	0.0005066035
1.0	0.9016536110	0.7592267250	0.5670032510	0.3172685870	0.0004854424
1.1	0.9089510180	0.7701010570	0.5778775830	0.3245659930	0.0006357846
Finite Difference Solution	0.8785241309	0.7393459703	0.5692353831	0.3489950759	-

Table 2. MSE for the second-order approximate solution of (9) using HAM at the various h values

h	X1 = 0.2	X2 = 0.4	X3 = 0.6	X4 = 0.8	MSE
0.1	0.8428694348	0.6716292313	0.4794116684	0.2584946524	0.0055288601
0.2	0.8562494747	0.6915693946	0.4993695636	0.271905424	0.0034007022
0.3	0.8688196658	0.7103038888	0.5181336138	0.284526834	0.0019262910
0.4	0.8805800078	0.7278327158	0.5357038158	0.296358881	0.0010079292
0.5	0.8915305008	0.7441558748	0.552080173	0.307401568	0.0005541555
0.6	0.9016711446	0.7592733636	0.567262682	0.317654891	0.0004797460
0.7	0.9110019404	0.7731851864	0.581251346	0.327118856	0.0007057133
0.8	0.9195228880	0.7858913410	0.594046165	0.335793457	0.0011593068
0.9	0.9272339846	0.7973918266	0.6056471356	0.343678697	0.0017740127
1.0	0.9341352338	0.8076866444	0.6160542620	0.3507745750	0.0024895541
1.1	0.9402266332	0.8167757940	0.6252675400	0.3570810934	0.0032518907
Finite Difference Solution	0.8785241309	0.7393459703	0.5692353831	0.3489950759	-
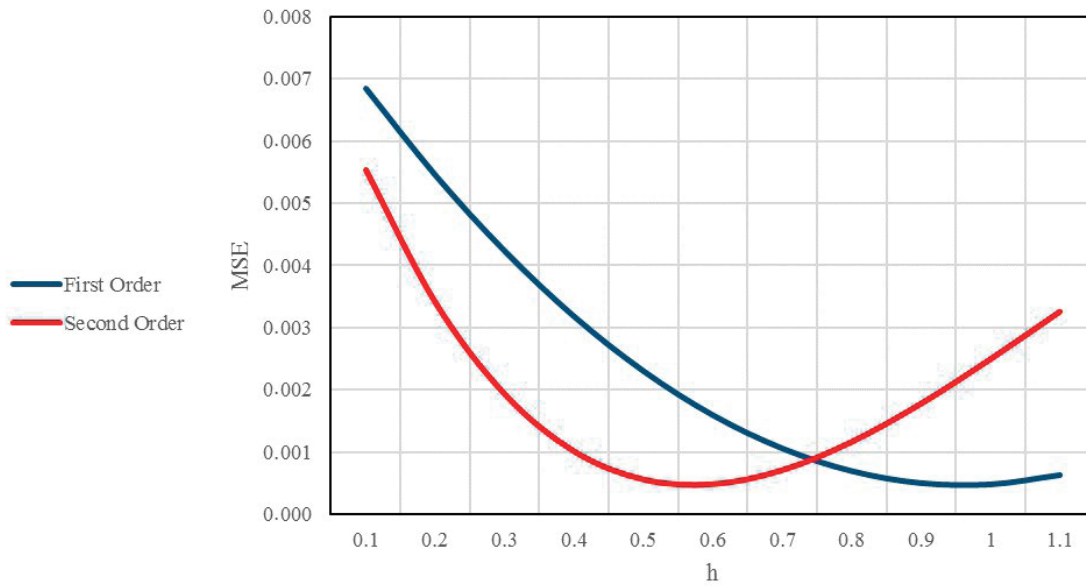
Figure 2. MSE for the first and second-order approximations according to the *h* values.

Table 3. The solution of (9) at $h = 1.0$, $\tau = 1$ with the minor values of ε

ε	X = 0.2	X = 0.4	X = 0.6	X = 0.8
$\varepsilon = 0.0$	0.931757074	0.803379825	0.61115635	0.347372048
$\varepsilon = 0.1$	0.931994893	0.803810506	0.61164614	0.347712304
$\varepsilon = 0.2$	0.932232706	0.804241189	0.61213593	0.348052554
$\varepsilon = 0.5$	0.932946156	0.805533236	0.61360531	0.349073312
$\varepsilon = 1.0$	0.934135235	0.807686645	0.61605426	0.350774575
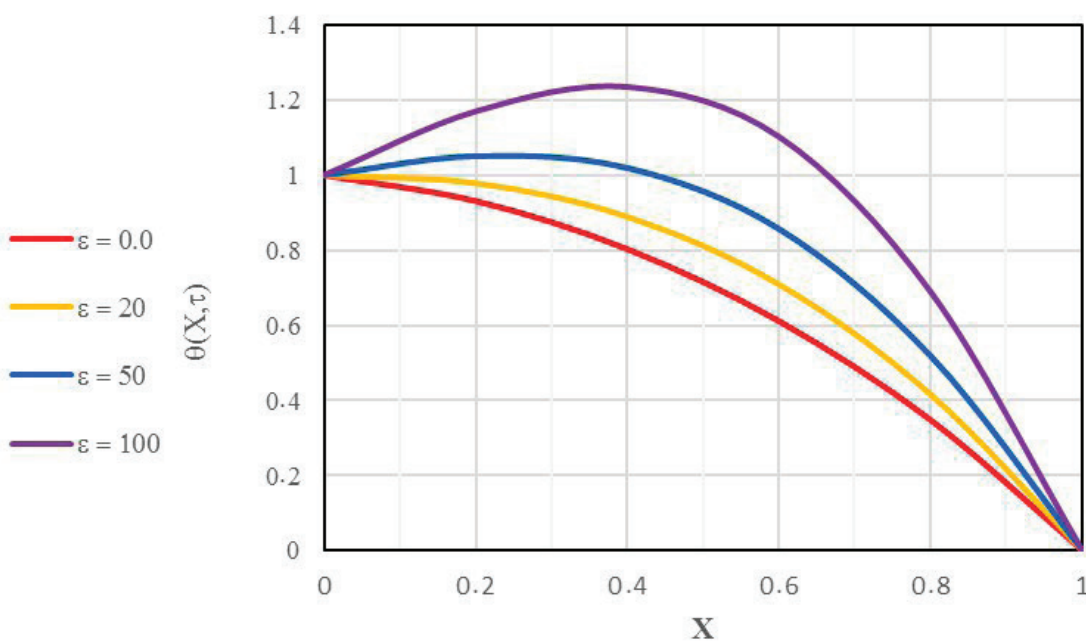
Figure 3. The second-order approximate solutions of (9) at $h = 1.0$, $\alpha_i = 1$ ($i = 1,2,3$), $\tau = 1$ with various ε values.
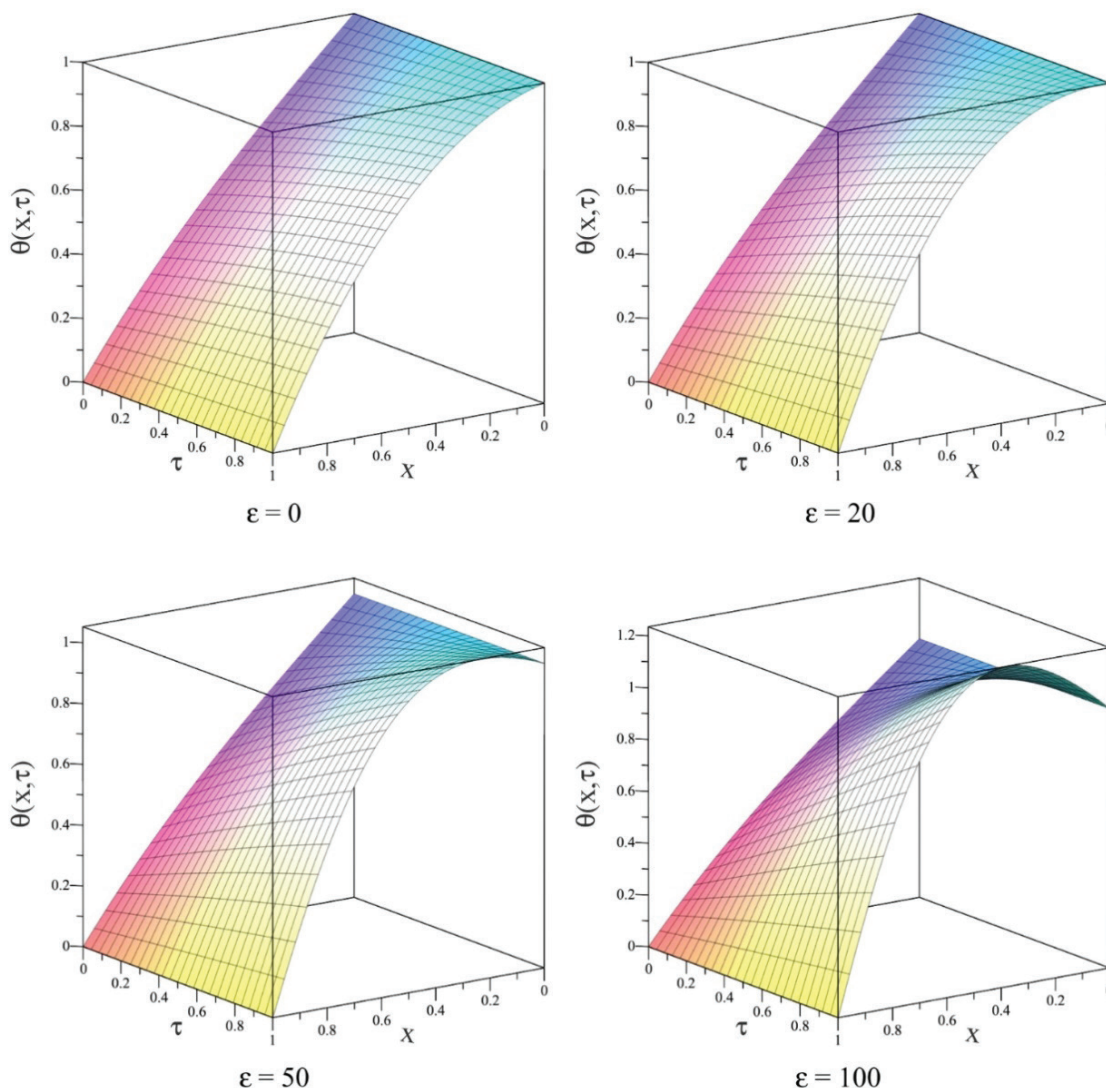
Figure 4. The second-order approximate solutions of nonlinear Pennes' bioheat equation at ε = 0, 20, 50, 100, α_i = 1.0 (i = 1,2,3), h = 1.0.

CONCLUSION

The comparison between the analytical answer of Pennes' equation arising from the Homotopy Analysis Method and the numerical solution demonstrates a very good agreement. It is not easy to obtain the high-order deformations of nonlinear Pennes' bioheat equation for the high computational cost of HAM; However, achieving the acceptable accuracy by applying the convergence-control parameter's optimum values even at the low-order approximations is possible. Analyzing the effect of ε on the solution indicates that the increase in this parameter's value will increase the temperature. Nevertheless, the effect is inconsiderable even for the large values of ε, thus it is reasonable to consider the specific heat capacity of a living tissue independent of its temperature (a constant value). Referring to this study, HAM is considered an appropriate analytical technique to compute the solution of Pennes' equation in a nonlinear form.

NOMENCLATURE

T	Temperature
t	Time
ρ_t	Density of tissue
c_t	Specific heat capacity
k	Thermal conductivity
ρ_b	Density of blood
c_b	Specific heat capacity of blood
ω_p	Blood perfusion rate
T_a	Core body temperature
q_m	Volumetric metabolic heat generation

AUTHORSHIP CONTRIBUTIONS

Authors equally contributed to this work.

DATA AVAILABILITY STATEMENT

The authors confirm that the data that supports the findings of this study are available within the article. Raw data that support the finding of this study are available from the corresponding author, upon reasonable request.

CONFLICT OF INTEREST

The author declared no potential conflicts of interest with respect to the research, authorship, and/or publication of this article.

ETHICS

There are no ethical issues with the publication of this manuscript.

REFERENCES

[1]   Pennes HH. Analysis of tissue and arterial blood temperatures in the resting human forearm. J Appl Physiol 1948;1:93–122. [CrossRef]

[2]   Hristov J. Bio-heat models revisited: Concepts, derivations, nondimensalization and fractionalization approaches. Front Phys 2019;7:00189. [CrossRef]

[3]   Shih TC, Yuan P, Lin WL, Sen Kou H. Analytical analysis of the Pennes bioheat transfer equation with sinusoidal heat flux condition on skin surface. Med Eng Phys 2007;29:946–953. [CrossRef]

[4]   Shahnazari, Aghanajafi, Azimifar. Investigation of bioheat transfer equation of pennes via a new method based on wrm & homotopy perturbation. 2014. Available at: https://api.semanticscholar.org/CorpusID:212596037. Accessed May 2, 2024.

[5]   Qin Y, Wu K. Numerical solution of fractional bioheat equation by quadratic spline collocation method. 2016. J Nonlinear Sci Appl 2016;9:5061–5072. [CrossRef]

[6]   Al-Humedi HO, Al-Saadawi FA. The numerical solution of bioheat equation based on shifted Legendre polynomial. Int J Nonlinear Anal Appl 2021;12:1061–1070.

[7]   Liu KC, Tu FJ. Numerical solution of bioheat transfer problems with transient blood temperature. Int J Comput Methods 2019;16:1843001. [CrossRef]

[8]   Singh J, Gupta PK, Rai KN. Solution of fractional bioheat equations by finite difference method and HPM. Math Comput Model 2011;54:2316–2325. [CrossRef]

[9]   Kumar P, Kumar D, Rai KN. A mathematical model for hyperbolic space-fractional bioheat transfer during thermal therapy. Procedia Engineer 2015;56:56–62. [CrossRef]

[10]   Wang X, Qi H, Yang X, Xu H. Analysis of the time-space fractional bioheat transfer equation for biological tissues during laser irradiation. Int J Heat Mass Transf 2021;177:121555. [CrossRef]

[11]   Kabiri A, Talaee MR. Analysis of hyperbolic Pennes bioheat equation in perfused homogeneous biological tissue subject to the instantaneous moving heat source. SN Appl Sci 2021;3:398. [CrossRef]

[12]   Irfan M, Shah FA, Nisar KS. Fibonacci wavelet method for solving Pennes bioheat transfer equation. Int J Wavelets Multiresolut Inf Process 2021;19:2150023. [CrossRef]

[13]   Irfan M, Shah FA. Fibonacci wavelet method for solving the time-fractional bioheat transfer model. Optik (Stuttg) 2021;241:167084. [CrossRef]

[14]   Lakhssassi A, Kengne E, Semmaoui H. Modified Pennes' equation modelling bio-heat transfer in living tissues: Analytical and numerical analysis. Nat Sci (Irvine) 2010;2:1375–1385. [CrossRef]

[15]   Gupta PK, Singh J, Rai KN. Numerical simulation for heat transfer in tissues during thermal therapy. J Therm Biol 2010;35:295–301. [CrossRef]

[16]   Majchrzak E. Numerical Solution of dual phase lag model of bioheat transfer using the general boundary element method. CMES Comput Model Engineer Sci 2010;69:43–60.

[17]   Majchrzak E, Turchan L. The general boundary element method for 3D dual-phase lag model of bioheat transfer. Engineer Anal Bound Elem 2015;50:76–82. [CrossRef]

[18]   Ostadhossein R, Hoseinzadeh S. The solution of Pennes' bio-heat equation with a convection term and nonlinear specific heat capacity using Adomian decomposition. J Therm Anal Calorim 2022;147:12739–12747. [CrossRef]

[19]   Ostadhossein R, Hoseinzadeh S. Developing computational methods of heat flow using bioheat equation enhancing skin thermal modeling efficiency. Int J Numer Methods Heat Fluid Flow 2023;34:1380–1398. [CrossRef]

[20]   Forghani P, Ahmadikia H, Karimipour A. Non-fourier boundary conditions effects on the skin tissue temperature response. Heat Transfer - Asian Research 2017;46:29–48. [CrossRef]

[21]   Akbari M, Hemmat Esfe M, Rostamian SH, Karimipour A. Non fourier heat conduction in a semi infinite body exposed to the pulsatile and continuous heat sources. J Curr Res Sci 2013;1:144–150.

[22]   Karimipour A, Hossein Nezhad A, D'Orazio A, Shirani E. Investigation of the gravity effects on the mixed convection heat transfer in a microchannel using lattice Boltzmann method. Int J Therm Sci 2012;54:142–152. [CrossRef]

[23]   Karimipour A, Taghipour A, Malvandi A. Developing the laminar MHD forced convection flow of water/FMWNT carbon nanotubes in

a microchannel imposed the uniform heat flux. J Magn Magn Mater 2016;419:420−428. [CrossRef]

[24] Karimipour A. New correlation for Nusselt number of nanofluid with Ag / Al2O3 / Cu nanoparticles in a microchannel considering slip velocity and temperature jump by using lattice Boltzmann method. Int J Therm Sci 2015;91:146−156. [CrossRef]

[25] Karimipour A, Alipour H, Akbari OA, Semiromi DT, Esfe MH. Studying the effect of indentation on flow parameters and slow heat transfer of water-silver nano-fluid with varying volume fraction in a rectangular two-dimensional micro channel. Indian J Sci Technol 2015;8:51707. [CrossRef]

[26] Menni Y, Azzi A, Chamkha A. Turbulent heat transfer and fluid flow over complex geometry fins. Defect Diffus Forum 2018;388:378−393. [CrossRef]

[27] Menni Y, Azzi A, Chamkha A. Modeling and analysis of solar air channels with attachments of different shapes. Int J Numer Methods Heat Fluid Flow 2019;29:1815−1845. [CrossRef]

[28] Menni Y, Azzi A, Chamkha A. Enhancement of convective heat transfer in smooth air channels with wall-mounted obstacles in the flow path: A review. J Therm Anal Calorim 2019;135:1951−1976. [CrossRef]

[29] Menni Y, Saim R. Numerical simulation of turbulent forced convection in a channel fitted with baffles of various shapes. Université Abou Bekr Belkaid de Tlemcen Faculté de Technologie Le 3ème Séminaire sur les Technologies Mécaniques Avancées, 8-9 November 2014.

[30] Liao S. Homotopy analysis method: A new analytical technique for nonlinear problems. Commun Nonlinear Sci Numer Simul 1997;2:95−100. [CrossRef]

[31] Chakraverty S, Mahato N, Karunakar P, Rao TD. Advanced Numerical and Semi-Analytical Methods for Differential Equations. Homotopy Analysis Method. Hoboken: Wiley; 2019. pp. 149−156. [CrossRef]

[32] Abbasbandy S. Homotopy analysis method for heat radiation equations. ICHMT 2007;34:380−387. [CrossRef]

[33] Hariharan G. A homotopy analysis method for the nonlinear partial differential equations arising in engineering. JCMSE 2017;18:191−200. [CrossRef]

[34] Gupta VG, Gupta S. Application of homotopy analysis method for solving nonlinear cauchy problem. Surv Math Appl 2012;7:105−116.

[35] Lu D, Liu J. Application of the homotopy analysis method for solving the variable coefficient kdv-burgers equation. Abstr Appl Anal 2014:309420. [CrossRef]

[36] Hesameddini E, Latifizadeh H. Homotopy analysis method to obtain numerical solutions of the Painlevé equations. Math Methods Appl Sci 2012;35:1423−1433. [CrossRef]

[37] Hammouch Z, Mekkaoui T, Sadki H. Homotopy analysis method for solving MHD free convection flow from a cooling sheet. Math Natural Sci 2019;3:39−47. [CrossRef]

[38] Odibat Z. An improved optimal homotopy analysis algorithm for nonlinear differential equations. J Math Anal Appl 2020;488. [CrossRef]

[39] Biswal U, Chakraverty S. Investigation of Jeffery-Hamel flow for nanofluid in the presence of magnetic field by a new approach in the optimal homotopy analysis method. J Appl Comput Mech 2022;8:48−59.

[40] Obalalu AM, Ajala AO, Akindele AO, Oladapo OA, Adepoju O, Jimoh MO. Unsteady squeezed flow and heat transfer of dissipative casson fluid using optimal homotopy analysis method: An application of solar radiation. Part Differ Equat Appl Math 2021;4:100146. [CrossRef]

[41] Rabbani M. Modified homotopy method to solve non-linear integral equations. Int J Nonlinear Anal Appl 2015;6:133−136.

[42] Jbr RK, Al-Rammahi A. Q-homotopy analysis method for solving nonlinear fredholm integral equation of the second kind. Int J Nonlinear Anal Appl 2021;12:2145−2152.

[43] Ahmad AA. Solving partial differential equations via a hybrid method between homotopy analytical method and Harris hawks optimization algorithm. Int J Nonlinear Anal Appl 2022;13:663−671.

[44] Huang HW, Horng TL. Bioheat transfer and thermal heating for tumor treatment. In: Becker SM, Kuznetsov AV, eds. Heat Transfer and Fluid Flow in Biological Processes. Amsterdam: Elsevier; 2015. pp. 1−42. [CrossRef]

[45] Ghanmi A, Abbas IA. An analytical study on the fractional transient heating within the skin tissue during the thermal therapy. J Therm Biol 2019;82:229−233. [CrossRef]

[46] Liao S. Beyond Perturbation. New York: Chapman and Hall/CRC; 2003. [CrossRef]

[47] Fürnkranz J. Encyclopedia of Machine Learning. Boston, MA: Springer US; 2010. [CrossRef]